Active and Passive Elec. Comp., 1989, Vol. 13, pp. 133–150
Reprints available directly from the publisher
Photocopying permitted by license only

AG-BASED THICK-FILM FRONT METALLIZATION OF SILICON SOLAR CELLS

M. PRUDENZIATI, L. MORO, B. MORTEN, F. SIROTTI
Department of Physics, University of Modena, Italy
L. SARDI
Ansaldo USE, Genova, Italy

(*Received April 14, 1988; in final form June 10, 1988*)

The evolution of microstructure and electrical properties of silver-based thick-film metallizations of silicon solar cells prepared by infrared firing processes has been investigated. The performance of the cells are shown to be dependent on several dynamical and diffusive phenomena. In particular, the sintering of silver grains, silver diffusion into the glass, and the flow of glass at the metal/silicon interface strongly affect important characteristics of the cells such as sheet and contact resistivities and the adhesion of fingers and bus bars. The existance of an optimum value of the peak firing temperature is observed and explained in terms of competitive phenomena occurring at the metal/silicon interface. Moreover it is shown that IR firing treatments require a careful consideration of the sequence of printing and firing steps. The features of heat treatments performed in conveyor belt furnances using Joule and infrared sources are compared.

INTRODUCTION

The advantages of thick film technology for solar-cell manufacture are well known[1–3]. Virtually all the processes required to prepare a silicon solar cell (dopant diffusion to create a junction, metal deposition for front and back contacts, AR coating, etc.) can be performed using this technology although contact-deposition is the most commonly adopted[1]. Main advantages of TFT for this purpose are low cost of materials, automation of processes, and stability and reliability of the contacts[3]. Nevertheless, thick-film metallized cells sometime show a lower efficiency than those prepared by thin film processes. On the other hand, the knowledge of basic phenomena involved in thick-film metallization is still unsatisfactory, and con-

siderable improvements are expected from a more systematic research in this field.

A thick-film-metallization ink contains the main metal and other constituents such as a glass frit and sometime other metal oxides. Silver is the most commonly used main constituent of inks for front contacts while Ag/Al based inks are usually employed for the back surface. These choices are due to compromises among basic requirements of good conductivity, low diffusivity into silicon, and good solderability.

Other constituents of the paste (glass frit and metal oxides) play a relevant role in the contact performance, particularly in achieving low series, high parallel resistance, and good adhesion with the silicon substrate.

The choice of the firing cycle for a given ink is usually based on instructions suggested by the ink manufacturer. Nevertheless, the final choice is determined by the particular facilities available and cell design by a trial and error approach. As a consequence information in the literature on the evolution of microstructure and electrical properties of thick film metal contacts on Si is fragmentary and partially contradictory[3–7].

This paper present the results of a study of front contacts prepared from Ag-based inks. The results illustrate the role played by different constituents of the ink and by the preparation processes in the evolution of microstructure and electrical properties of the cells.

SAMPLE PREPARATION

Solar cells were prepared from (100) single crystal wafers of silicon p-type (boron-doped) having a resistivity into the range 0.5–5 ohm.cm. Although results of this study equally apply to polysilicon wafers, single-crystal cells were more suitable for analytical investigation. The original wafers, 4″ in diameter and 300 μm thick were $POCl_3$ diffused at 850°C, 25′ in order to obtain a n+/p junction at about 3000 Å below the surface.

Thick-film metallizations were prepared using a silver/aluminum-based ink (4902 DuPont) on the back and a Ag-based ink (TFS 3347) on the front of the cells. The first step was back-metallization printing. After drying at about 200°C, the front metallization was deposited and the wafers were fired in a conveyor infrared furnace

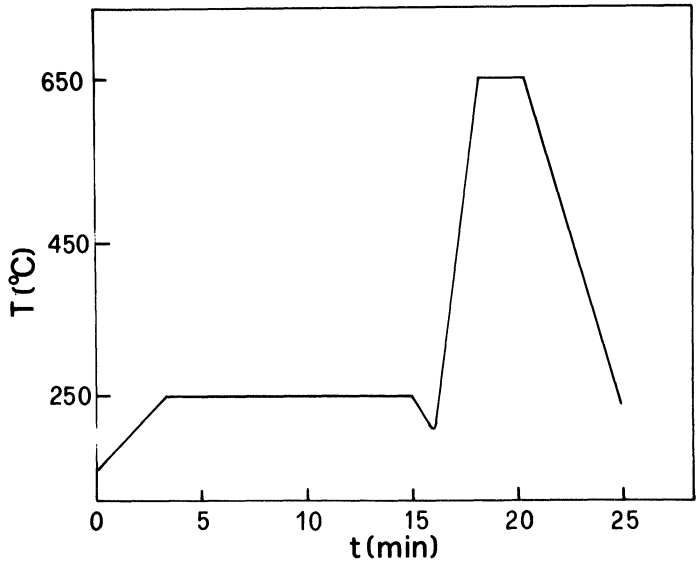

FIGURE 1 A typical temperature profile for infrared firing of silicon solar cells.

(Radiant Technology Corporation, C-500 A). Figure 1 shows a typical firing profile. Peak temperature was changed as a parameter in the range 450°C to 750°C, by steps of 50°C.

Samples were also prepaked without back metallization.

EXPERIMENTAL METHODS

A scanning electron microscope (Philips PSEM-500 PX) equipped with an X-ray energy dispersive spectrometer (EDAX-9100) was used for metallurgical and elemental investigation. The EDAX system, allows a semiquantitative evaluation of detectable elements ($Z > 9$) with a sensitivity of 0.1% for bulk materials and the collection of distribution maps for a chosen element in the sample. The accuracy in the concentration analysis was limited by thick film morphology.

Insight on metal-silicon interactions was obtained by SEM observations of sample surfaces after selective chemical etchs. In order to remove Ag from metal layers the samples were immersed in a solu-

tion of ammonia (25%) and H_2O_2 (10 vol.), 1:1 in volume. Etching time was about 20 hours.

Some samples were cleaved after a quick extraction from a liquid nitrogen bath in order to obtain very sharp cross sections enabling us to investigate metal-Si interactions and depth morphology.

Metallization-thickness measurements were performed using a Taylor-Hobson Talysurf 10. Standard photovoltaic response of cells under AM1 illumination was measured. Electrical properties of metal layers (sheet resistance) and devices (diffusion layer sheet resistivity, contact resistance) were studied using the test pattern illustrated in Figure 2[8]. Finally, contact adhesion was evaluated in terms of the force required to peel off from the silicon surface small pads (5×5 mm^2) of contacts on which a tinned copper strip was soldered.

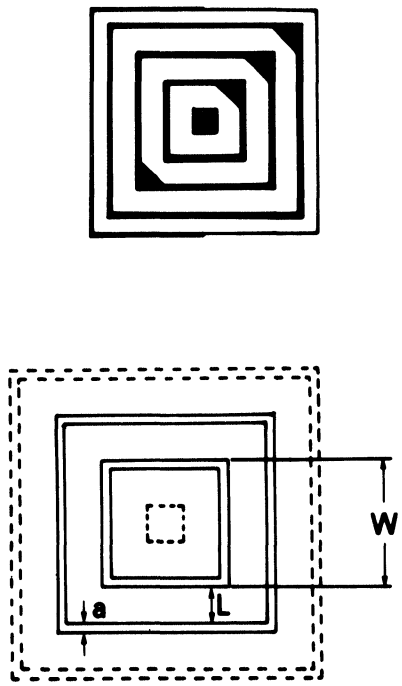

FIGURE 2 Test pattern for the measurement of metal sheet resistance and contact resistance; d = 0.25 mm, L = 0.90 mm, W = 2.8 mm.

RESULTS

Inks

Analysis of the inorganic constituents of unfired ink shows that the Ag content is about 90% by weight of the detectable elements. Other detected elements are typical components of a glass; Pb with the greatest concentration as well as considerable amounts of Si and Al.

Figure 3 shows dispersed particles of the ink (a) and distribution maps of Ag and Pb (b and c). Ag particles are present in the ink as both spherical grains and flat compact flakes. Most of spherical particles are agglomerated, and their mean size is estimated as .5 μm, while flakes dimensions are in the range of 2–4 μm. Diaphanous flakes, a few microns large, are also evident. They were identified by elemental analysis as glass frit particles; a result confirmed by the Pb distribution map.

Layers

Thermal treatments induce changes in the microstructure and morphology of printed layers due to the following processes: shrinking of the layers, evident from a decrease in thickness with an increase of the peak temperature T_f (Figure 4); sintering of the Ag particles, as observed by SEM (Figure 5); glass flow down to the silicon surface (Figure 6).

Particles of glass frits are visible on the printed layers up to T_f = 450°C, but can not identified on samples fired at 550°C. These results suggest that the transition temperature of the glass lays in the range between 500 to 550°C. Sintering of Ag grains and flakes starts in this range of temperatures, in standard processes with back deposition present.

Figure 5a compares the surfaces of metal-layers fired at 500°C. Sample (a) is prepared with a front contact by a standard process, while in sample (b) the back layer is lacking. Observed in these micrographs is a delay in sintering for sample (b), as well as the lower shrinking of the fingers and bus bars at the same T_f when cells are prepared in absence of the back deposition (Figure 4). Let us now restrict ourselves to the standard process.

Incipient sintering of metal particles can be observed on sample (a) fired at 550°C. Some necks between particles are present, but

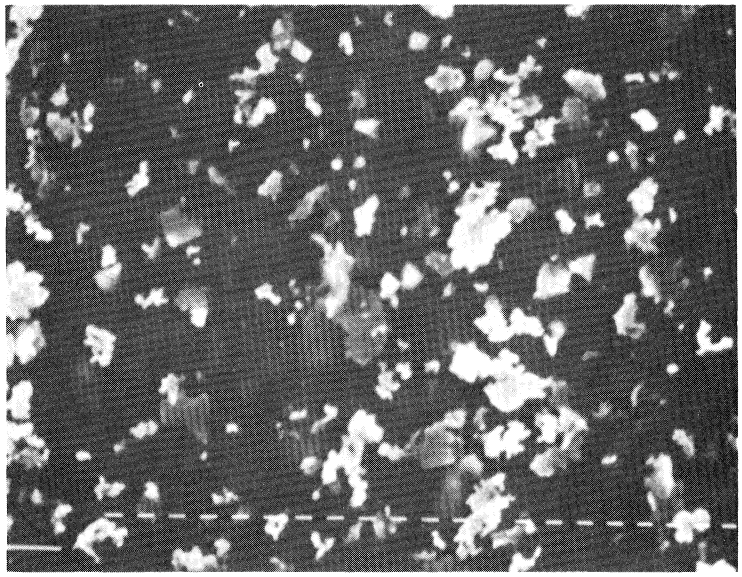

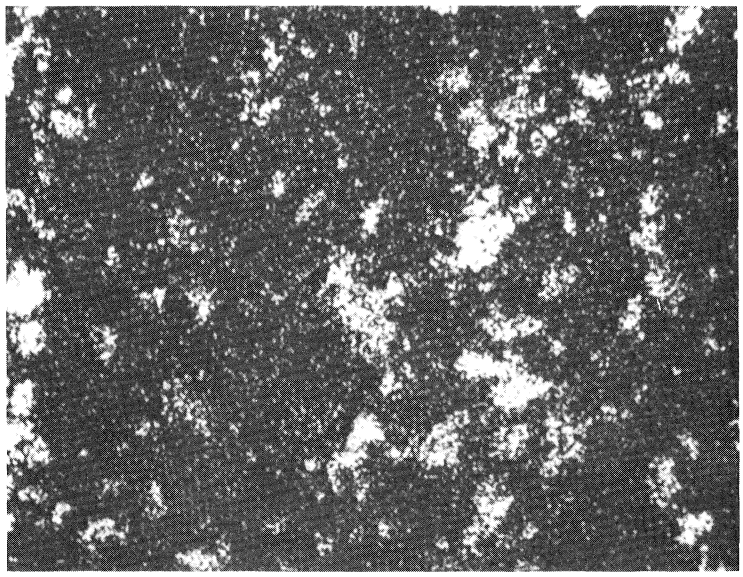

FIGURE 3 a) SEM picture of the inorganic components of the Ag-based ink TFS 3347. b) EDS map of silver and c) lead.

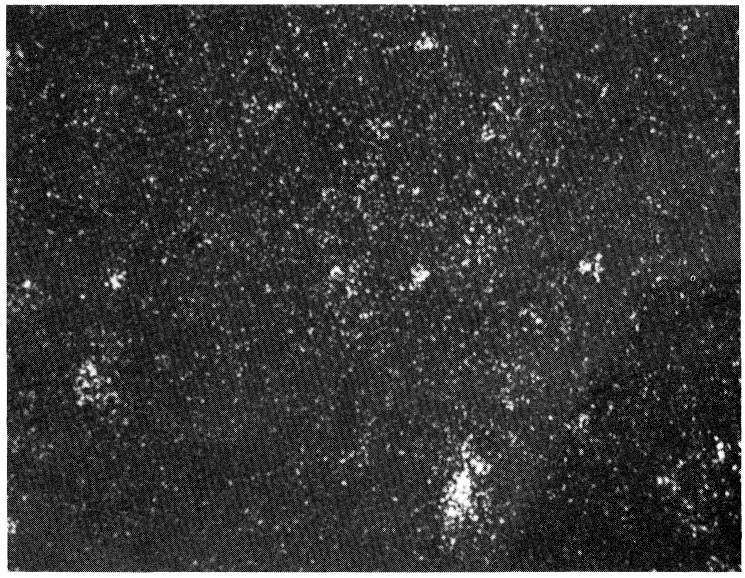

C

FIGURE 3 (*Contd*)

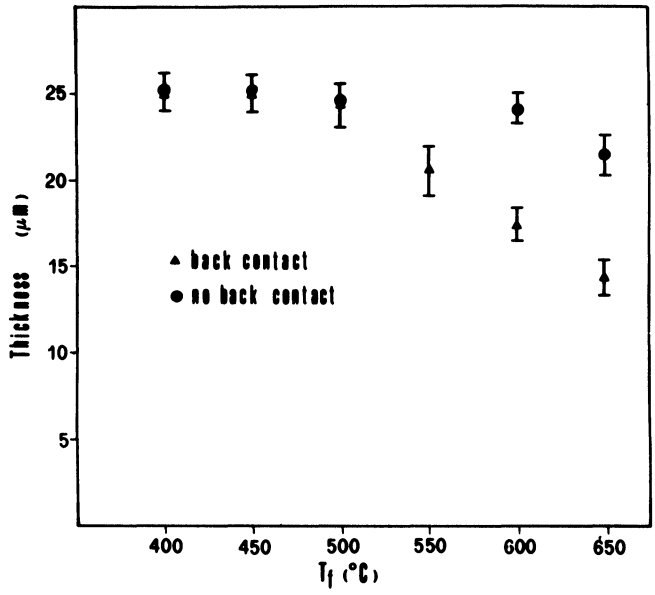

FIGURE 4 Shrinking of the Ag-metal layer by increasing the peak firing temperature with and without the back contact deposition.

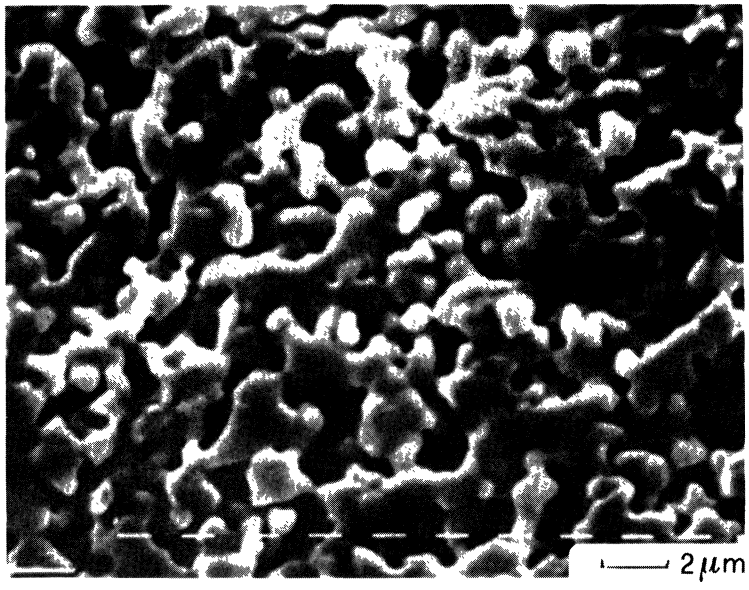

FIGURE 5 SEM picture of the Ag front metal layer prepared in the same firing conditions, T_f = 600°C, except for the presence (a) and absence (b) of the back contact layer.

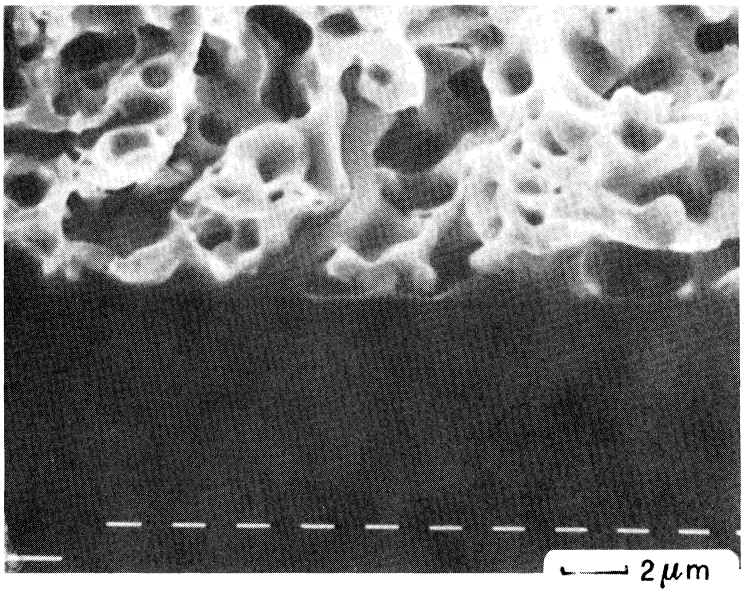

FIGURE 6 SEM picture of the cross section of the interface between the Ag-metal and the silicon substrate; T_f = 650°C.

most of metal grains keep their individuality and the mean sizes are unchanged. Also observed are glassy flakes on metal particles that are roundish in appearance.

Heat treatment at 600°C allows sheet formation: necks between particles increase and grains lose their individuality to form a continuous layer.

A positive correlation exists between the behavior of thickness change and the sintering of grains as observed by SEM analysis.

DISSOLUTION OF SILVER IN GLASS BINDER

In a parallel investigation[9] we studied diffusion and solubility of silver in seven lead glasses of different compositions. We found that dissolution of Ag occurs via thermally activated diffusion processes characterized by relatively high diffusion coefficients D, in the range of 10^{-12} to 10^{-11} m^2 sec^{-1} at 850°C and activation energies in the

range from 1 to 1.5eV (according to the composition of the glass). Higher boron content and/or lower silicon content were associated with higher diffusivities of Ag.

Moreover relatively high solubilities of Ag were found. For example in a glass with the composition 55.5% PbO, 10.5% SiO_2, 22% B_2O_3, 12% Al_2O_3 by weight, 2.5% Ag was dissolved at 850°C and 10.2% was dissolved at 1000°C. Similarly a glass with the composition 59.9% PbO, 22% SiO_2, 19% B_2O_3 dissolved about 2.04% Ag at 850°C and 8.5% at 1000°C.

We did not try to get quantitative data on solubilities in samples prepared at lower temperatures because this analysis would require analytical methods of higher sensitivity and better spatial resolution than that available. However, the extrapolation of the data collected at the temperatures of interest for the present case (600°C to 700°C), also shows that in these conditions, a firing process lasting for a few minutes is able to saturate a layer less than a micrometer thick with several hundreds ppm of silver atoms. As a consequence the glassy layer interfacing the silver metallization with the silicon substrate has to be considered a "heavily doped" glass.

SUBSTRATE/LAYER INTERFACE

The buried layer/silicon interface is exposed to analysis by means of the above mentioned chemical etch, which dissolves away Ag-metal but does not affect the glass binder. A typical micrograph of the wafer surface under a finger prepared in this way is shown in Figure 7. The wavelike reliefs pertain to a glassy film covering all the Si wafer surface, since elemental analysis detects Pb, the main constituent of the glass binder. The thickness of this film, for T_f = 600°C in standard conditions, is about 1 μm on the highest "hillocks" that cover a large fraction of the underlaying silicon surface.

Both the area covered by "thick glassy film" and the heights of the "hillocks" increase by increasing the firing temperature. A qualitative evaluation of these two quantities is illustrates in Figure 8. In this interfacial glassy film, EDS analysis shows the presence of dissolved Ag, in agreement with the results presented in the previous section.

A correlation between the formation of the glassy interfacial film and the adhesion of the contact is found. Figure 9 shows that the

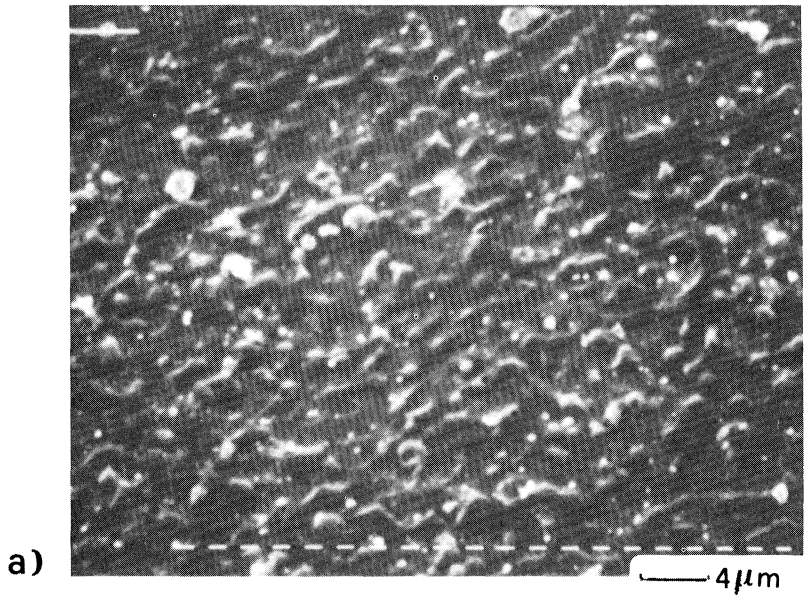

FIGURE 7 Surface of the silicon cell under a bus bar, after the removal of the front contact by means of chemical etching. a) 2500 X, b) 5000 X.

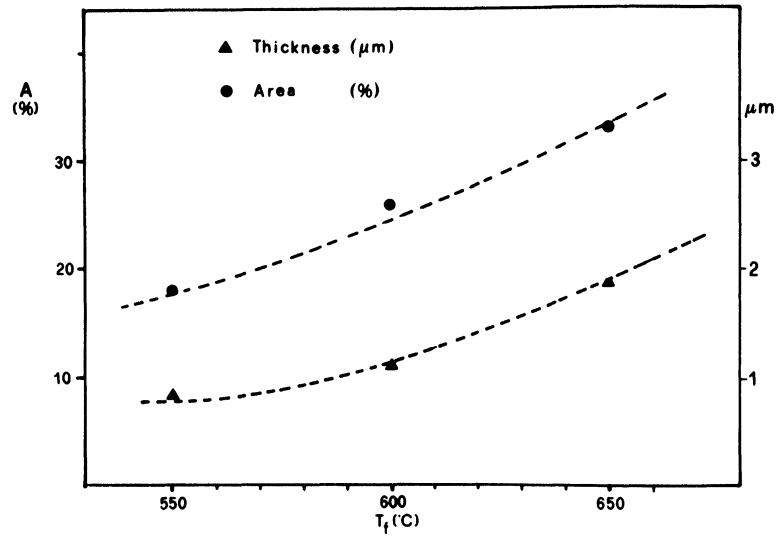

FIGURE 8 Change of heights of highest hillocks (right scale) and mean coverage area of the same hillocks (left scale) of the surface glass layer on silicon, as a function of the peak firing temperature.

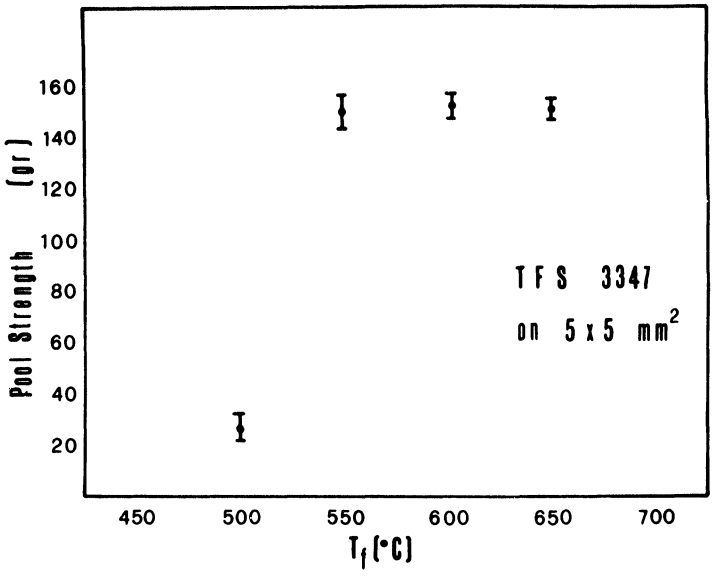

FIGURE 9 Adhesion behavior of silver metal contacts vs the peak firing temperature.

adhesion strength, negligible for T_f = 500°C, reaches a nearly constant value when T_f = 550°C, i.e. the temperature corresponding to the formation of a glassy film covering the most part of the Si/metal interface.

ELECTRICAL PROPERTIES

Figure 10 shows the dependence of contact resistance R_c and metal sheet resistance R_l on the peak firing temperature. R_l monotonically decreases in the low temperature range and becomes nearly constant at higher temperatures. This result can be related to the behavior of sintering and shrinking of the metal layer in a comparison of Figures 9, 4 and 5. On the other hand, the contact resistance as a function of the peak firing temperature exhibits a minimum close to 650°C. The I–V characteristics of the cells under AM1 exposure are shown in Figure 11. The high series resistance of the cells prepared at low

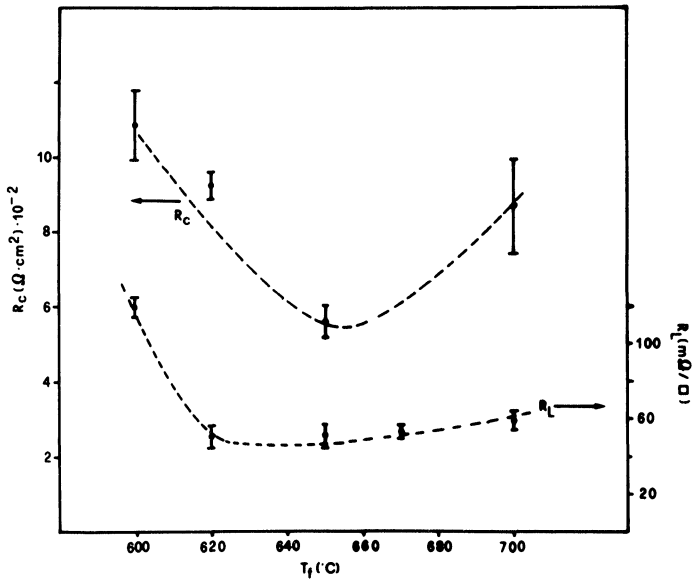

FIGURE 10 Sheet resistance R_l and contact resistivity R_c of the front contact of cells prepared at different peak firing temperatures.

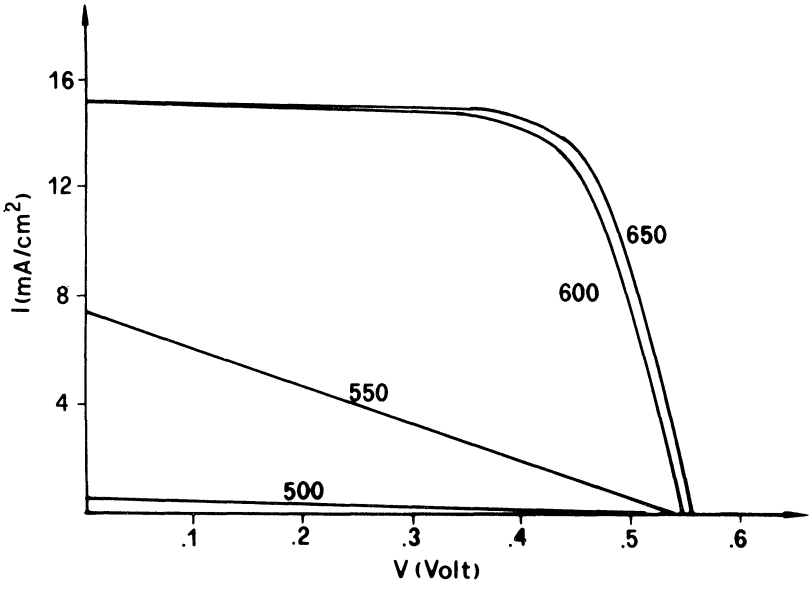

FIGURE 11 I–V characteristics of solar cells under AM1 exposure. Cells were not provided with A_r coatings.

temperatures are clearly related, with high values of both R_l and R_c, while the very good fill factor of the cells prepared at 650°C can be associated with the minimum R_c value.

DISCUSSION AND CONCLUSIONS

We have analyzed the evolution of the microstructure of Ag-based thick-film front contacts of Si solar cells as well as the related evolution of electrical and adhesion properties. Evidence has been found for: the formation of a glassy interfacial layer due to flow of the glass binder; dissolution of Ag-metal into this glass; a minimum of the contact resistance; and a considerable effect of the processes steps on the formation of the front contacts.

These findings enable us to describe and predict, in a general way, how preparation processes and material properties affect the cell performance.

In thermal treatments in conveyor belt furnances operating by the Joule effect, the heat exchanges are mainly through thermal convection and conduction, while radiation plays a negligible role. In fact, radiation is involved only during the short-time interval which lasts between the entrance of the material into the hot zone of the muffle and the time when it has been heated up at a temperature nearly equal to that of the muffle walls. If T_c (e.g. 300°C) represents the temperature of the material preheated in the drying zone and T_p (e.g. 650°C) the peak temperature of hot (firing) zone, the temperature gradient ($T_p - T_c$) between the source (muffle) and the body is relatively low, and so is the heat Q exchanged by radiation. Moreover, as long as the body heats up by means of thermal convection (the furnace atmosphere) and conduction (being in contact with the heated belt), Q decreases to a null value.

The process is quite different in IR furnaces. Here the temperature T_s of the source is considerably higher (e.g. 1300°C) than both T_c and T_p[10]. Hence, the radiation-transferred energy Q is much higher, and the exchange occurs during the whole path of the sample into the furnace. These high Q values enable fast firing cycles, which in turn make the heat exchange by conduction and convention negligible. On the other hand, the absorption of radiant heat is dependent on the "optical" properties of the body, which should be a "black body" in order to have maximum absorption. A Si wafer, 300–400 μm thick, largely differs from a black body in the range of radiation wavelengths generated by a IR source. In fact, typical IR furnaces emit a spectrum of radiation between .5 to 4.5 μm, with a maximum power near 1.8 μm[11]. In these spectral regions, the absorption coefficient of Si is very low[12], so that a large part of the incident radiative energy is lost (Figure 12a). However, when the silicon wafer is covered by the back contact, the contact traps the radiative heat on the cell, since it behaves like a "mirror" for IR radiation (Figure 12b). In our experimental conditions, we found that both Ag and Al (the main constitutents of the back contact) exhibit a high reflectivity at the radiation wavelengths of interest. In this way, the radiation heat is dispersed, and a large fraction of thermal energy contributes to activate the phenomena (glass flow, sintering, dissolution, etc) which are relevant to the formation of the front contact.

A more detailed and quantitative analysis of these phenomena would require complex simulations of heat exchange processes. How-

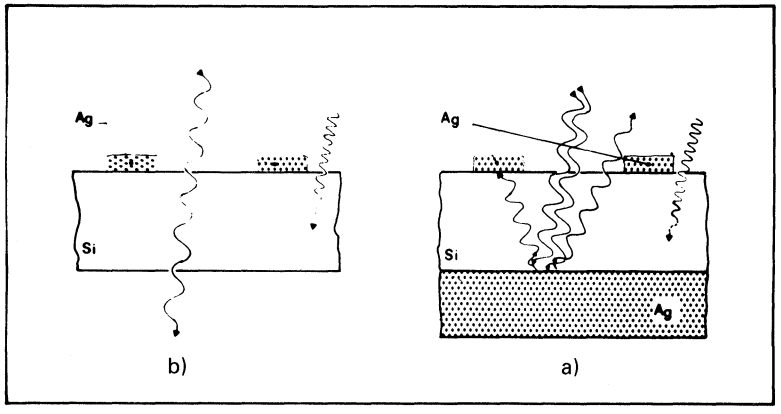

FIGURE 12 Sketch of the absorption and reflection processes of radiation incident on a Si wafer with front metal deposits a) with printed back contact, b) without the back contact.

ever the previous simple considerations suffice to understand the results reported in the previous sections (Figures 4 and 5).

For the front metal formation, we have to take into account the following cooperative phenomena, generally occurring in the indicated temperature ranges:

a) evaporation and pyrolysis of the organic vehicle ($T < 400°C$)
b) sintering of Ag particles (500–650°C)
c) glass percolation through the porous metal layer and coverage of the silicon surface with a thin glass film ($T \geq 500–650°C$)
d) Ag dissolution in the glass binder

The phenomenon at point b) is mainly responsible for the sheet resistance of fingers and bus bars (R_l in Figure 10). The adsorbed heat promotes the sintering up to a maximum stage, where the minimum value of R_l is reached. The phenomena at point c) are mainly responsible for the contact adhesion (Figures 6 and 9) but greatly affect also the contact resistance (Figure 10). We have found that for adequate adhesion, heat treatments at relatively low temperatures are sufficient, and the pull strength does not increase by increasing T_f over 550°C, or in other words, by increasing thickness and area of the interfactial glassy layer on the Si wafer. Conversely the contact resistance R_c is greatly affected by the interfacial glassy film properties

which are related to the phenomena outlined in c) and d). The experimental evidence of a minimum value of R_c is consistent with the evolution of the microstructure of the front contact if we assume that electron tunneling is responsible for the electrical transport from Ag metal particles to Si through the interfacial glassy layer. At low temperatures, the interfacial layer is thinner on average but less transparent to electrons because of a small content of dissolved Ag. At intermediate temperature the best compromise between thickness and dissolution of Ag occours. At higher firing temperatures the increased "doping" of the glass is not enought to compensate for the higher thickness of the glass film.

This analysis explains why the glass binder is so critical for the cell performance. The glass composition affects the transition temperature and the viscosity vs temperature dependence, as well as the diffusivity and solubility of Ag into the glass. Moreover, the amount of glass binder affects the Ag wetting and sintering as well as the thickness of the glassy film at the Si/layer interface.

In conclusion, our study has pointed out the main phenomena responsible for the formation of Ag-based thick-film metallizations and the interplay between material properties, preparation processes, and cell performance. Our findings could form the basis for further improvements of inks and processes for high-efficiency, reliable, low-cost solar cells.

AKNOWLEDGEMENTS

This work was partially supported by the National Research Council of Italy under contract PFE-ENEA n. 233.1985 (Special Project on Energy).

The work of one of us (LM) was also supported by a grant of Ansaldo S.p.A., Italy. We are indebted to the staff of CIGS (Centro Interdipartimentale Grandi Strumenti) of the University of Modena, for assistance in SEM and EDS experiments and to Drs. E. Argentino and C. Jachetti (Chimet, Arezzo, Italy) for the preparation of glass inks for the study of silver dissolution.

REFERENCES

1. G.C. Dubey "Applications of thick film techniques to the manufacture of solar cells" Solar Cells *15*, 1–25 (1985).
2. K.R. Bube, V.K. Kapur, C.F. Gay and K.J. Lewis "Thick-film metallization of solar cells, A progress report" Intl. J. Hybrid Microel. *4*, 13–18 (1981).

3. G.C. Cheek, R.P. Mertens, R. Van Overstraeten, L. Frisson "Thick-film metallization for solar cell applications" IEEE Trans. *ED-31*, 602–609 (1984).
4. K. Firor and S. Hogan "Effects of processing parameters on thick film inks used for solar cell front metallization" Solar Cells *5*, 87–100 (1981–82).
5. L. Sardi, B. Bargioni, C. Canali, P. Davoli, M. Prudenziati, V. Valbusa "Some features of thick-film technology for solar cells back metallization" Solar Cells *11*, 51–67 (1984).
6. K. Firor, S.J. Hogan, J.M. Barrett and R.T. Coyle "Series resistance associated with thick-film contacts to solar cells" Proc. 16th IEEE Photovol. Spec. Conf. 824–827 (1982).
7. H.C. Lin, D.P. Spittlehouse and Y.W. Hsueh "Contact resistance of silver inks on solar cells" in Proc. 13th IEEE Photovoltaic Specialists Conf. 593–596 (1978).
8. D.E. Riemer "Evaluation of thickfilm material for use as solar cell contacts" Proceed. 13th IEEE Photovoltaic Specialists Conf. 603–608 (1978).
9. M. Prudenziati, B. Morten, F. Cilloni, A. Tombesi. In preparation.
10. J.L. Resutek, R.E. Cote' "Infrared firing of thick film compositions" Sol. State Technol. *24*, 39–43 (June 1981).
11. D.F. Flattery "Infrared firing of base-metal compositions" Int. J. Hybrid Microel. *5*, 460–465 (1982).
12. W.C. Dash, R. Newman "Intrinsic optical absorption in single crystal germanium and silicon at 77 K and 300 K" Phys. Rev. *99*, 1151–1155 (1955).
13. H.B. Briggs "Infrared absorption in silicon" Phys. Rev. *77*, 727–728 (1950).